(1968).
(64) V. M. Potapov, V. M., Dem'yanovich, and V. P. Zaitsev, *Dokl. Akad. Nauk SSSR*, **223**, 875 (1975); *Dokl. Chem. (Engl. Transl.)*, 447 (1975).
(65) V. M. Potapov, V. M., Dem'yanovich, and V. P. Zaitsev, *Zh. Org. Khim.*, **12**, 1689 (1976); *J. Org. Chem. USSR (Engl. Transl.)*, 1662 (1976).
(66) These compounds are all (+) and probably of *S* configuration, and we will label them as such henceforth.
(67) The vertical lines denote boundaries of the dyad.
(68) P. J. Flory, P. R. Sundararajan, and L. C. DeBolt, *J. Am. Chem. Soc.*, **96**, 5015 (1974).
(69) R. Fletcher, Harwell Subroutine Library, Routine VA10A; R. Fletcher, A.E.R.E. Report R.7125 (1972).
(70) A. T. Bullock, G. G. Cameron, and P. M. Smith, *Makromol. Chem.*, **176**, 2153 (1975).
(71) Reference 25, Chapter VI.
(72) P. J. Flory, *Macromolecules*, **7**, 381 (1974).
(73) T. Tsuruta, R. Fujio, and J. Furukawa, *Makromol. Chem.*, **80**, 172 (1964).
(74) A. Allio and P. Pino, *Helv. Chim. Acta*, **57**, 616 (1974).
(75) L. Merle-Aubry, Y. Merle, and E. Selegny, *Makromol. Chem.*, **176**, 709 (1975).
(76) V. P. Privalko and Y. S. Lipatov, *Makromol. Chem.*, **175**, 641 (1974).
(77) V. P. Privalko, *Polym. J.*, **7**, 202 (1975).
(78) Reference 25, Chapter III.
(79) J. A. Guest, K. Matsuo, and W. H. Stockmayer, private communication.
(80) A. Abe, *Polym. J.*, **1**, 232 (1970); *J. Polym. Sci., Polym. Symp.*, **No. 54**, 135 (1976); *Macromolecules*, **10**, 34 (1977).
(81) W. L. Mattice, *Macromolecules*, **8**, 644 (1975); **9**, 48 (1976); **10**, 511, 516, 1171 (1977).
(82) E. Saiz, J. E. Mark, and P. J. Flory, *Macromolecules*, **10**, 967 (1977).

Flat-Band Potential of n-Type Semiconducting Molybdenum Disulfide by Cyclic Voltammetry of Two-Electron Reductants: Interface Energetics and the Sustained Photooxidation of Chloride

Lynn F. Schneemeyer and Mark S. Wrighton*

Contribution from the Department of Chemistry, Massachusetts Institute of Technology, Cambridge, Massachusetts 02139.
Received February 17, 1979

Abstract: Cyclic voltammetry has been used to locate the band edges of n-type MoS_2 in CH_3CN/ and EtOH/$[n\text{-}Bu_4N]ClO_4$ solutions. The crucial experiments concern the study of the cyclic voltammetry of biferrocene (BF) and *N,N,N′,N′*-tetramethyl-*p*-phenylenediamine (TMPD) each of which has two, reversible, one-electron waves at Pt. At MoS_2, the first oxidation is reversible in the dark, whereas the second oxidation is observed only upon illumination of the MoS_2. The dark oxidation $BF \rightarrow BF^+$ and the photoanodic $BF^+ \rightarrow BF^{2+}$ are separated by only ~150 mV, allowing us to assign an uncommonly accurate flat-band potential of +0.30 + 0.05 V vs. SCE to MoS_2. This flat-band potential reveals that the valence band edge is at ca. +1.9 V vs. SCE showing that photooxidations workable at TiO_2 are thermodynamically possible at illuminated MoS_2 as well. As an example of the ruggedness of MoS_2, we demonstrate the ability to effect the sustained oxidation of Cl^- at illuminated n-type MoS_2. Conclusions from BF are fully supported by those from TMPD and one-electron systems ferrocene, acetylferrocene, 1,1′-diacetylferrocene, and $[Ru(2,2'\text{-bipyridine})_3]^{2+}$. Oxidation of $[Ru(2,2'\text{-bipyridine})_3]^{2+}$ can be effected >0.5 V more negative than at Pt by illumination of MoS_2.

We wish to report an exceptionally well-defined flat-band potential, E_{FB}, for n-type semiconducting MoS_2 in nonaqueous electrolyte solution. The procedure used follows from that outlined by Bard and his co-workers[1-3] for locating energy levels of semiconductors relative to the potentials of various redox couples by cyclic voltammetry. Locating the energy levels for MoS_2 is useful since MoS_2 has attracted interest recently as a photoelectrode material with a small band gap, E_{BG} = 1.75 eV, and having unusual ruggedness with respect to photoanodic decomposition.[4] The material has a layered geometrical structure leading to an electronic (band) structure which is consistent with a lowest optical absorption associated with Mo d bands. Most other n-type semiconducting photoanodes that have been studied involve p-band materials.[5] The durability of the n-type MoS_2 photoelectrode has been associated with the fact that the electronic excitation does not involve a transition having $S^{2-} \rightarrow$ Mo(IV) charge-transfer character. In a material such as CdS, optical excitation involves considerable $S^{2-} \rightarrow$ Cd(II) charge transfer, and photoanodic decomposition is a typical result. Our measurements establish what reductants can be photooxidized by illumination of n-type MoS_2. Quite interestingly, we find that the uphill oxidation of Cl^- can be sustained by illumination of n-type MoS_2 in CH_3CN solvent.

Scheme I. Energy Levels of n-Type MoS_2 at the Flat-Band Potential $E_f = E_{FB}$ Relative to the Positions of Various Redox Couples in CH_3CN Solution

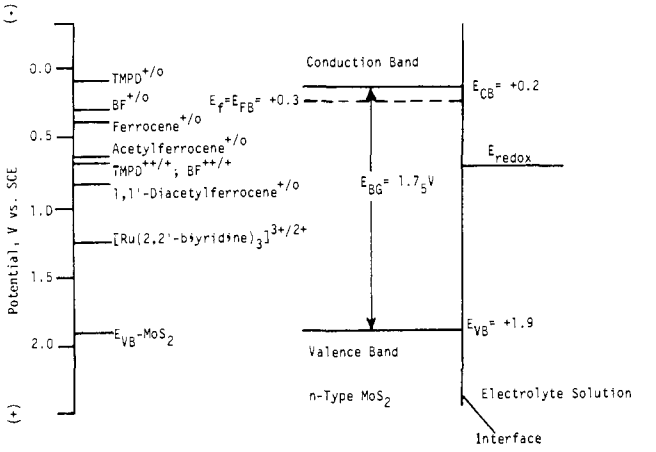

Results and Discussion

Determination of Flat-Band Potential of n-Type MoS_2. Cyclic voltammetry has been used to locate the band edges for

0002-7863/79/1501-6496$01.00/0 © 1979 American Chemical Society

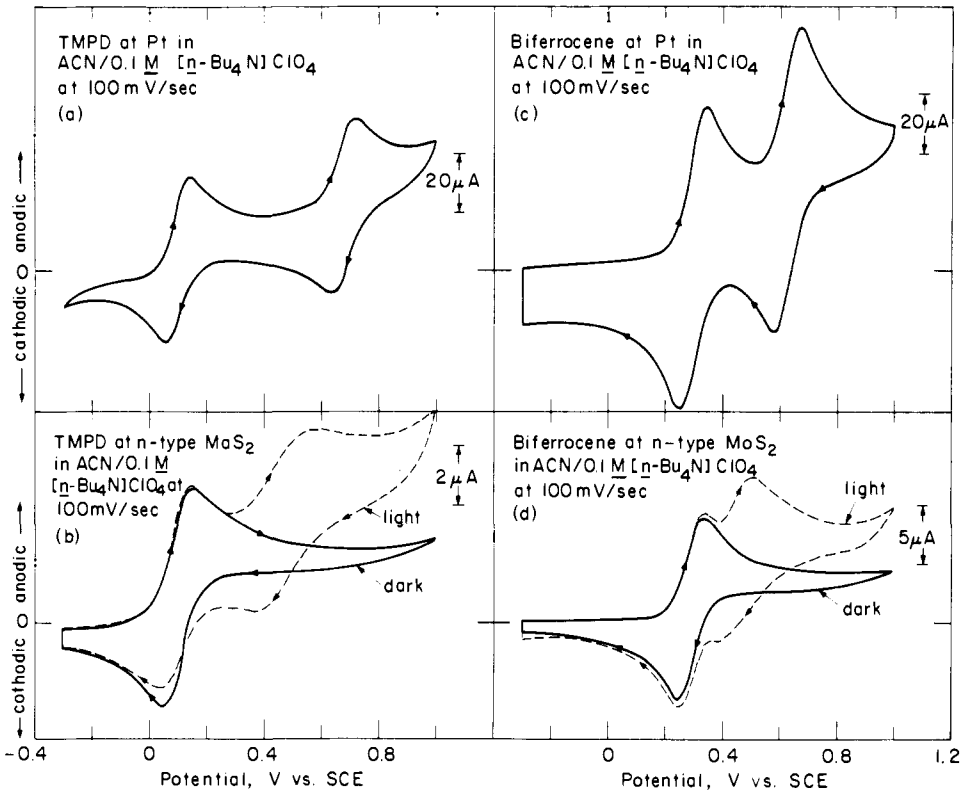

Figure 1. Comparison of cyclic voltammetry for TMPD (a and b) and biferrocene (c and d) at Pt and MoS_2 (dark or illuminated). Illumination was with 632.8-nm light at ~50 mW/cm^2.

n-type MoS_2 in CH_3CN or EtOH solutions of $[n\text{-}Bu_4N]ClO_4$. Scheme I includes some of our essential findings in this work. The value E_{FB} is that electrode potential, E_f, at which the bands are not bent. Scheme I[6] and the evaluation of this potential allow location of the valence and conduction band edges, E_{VB} and E_{CB}, respectively, by knowing E_{BG} and recognizing that E_{FB} is within 0.1 V of the conduction band. Locating E_{VB} reveals what solution reductants are thermodynamically capable of being oxidized by a photogenerated hole which rises to the top of the valence band (E_{VB}). For solution couples A^+/A where $E°$ falls within the conduction band, more negative than E_{CB}, the electrode should behave as if it were a reversible electrode,[1-3] whereas for $E°$ between E_{VB} and E_{CB} the n-type semiconductor should be blocking to oxidation. But irradiation of the semiconductor with light of energy $\geq E_{BG}$ should create holes which can oxidize $A \rightarrow A^+$ for any E_f positive of E_{FB} such that sufficient band bending exists to prevent back electron transfer. Thus, A can be photooxidized in an uphill sense to an extent equal to the difference in E_{FB} and $E°(A^+/A)$; that is, in Scheme I oxidation of the reduced component of the solution can be effected at electrode potentials, E_f, more negative than E_{redox} but E_f must be more positive than E_{FB}.

Cyclic voltammetry for a two-electron system A^+/A and A^{2+}/A^+ where the $E°$'s are different is particularly valuable and especially so if one $E°$ is in the conduction band and the other is in the "stateless gap" between E_{VB} and E_{CB}. For MoS_2 both *N,N,N',N'*-tetramethyl-*p*-phenylenediamine (TMPD) and biferrocene (BF) meet this criterion; Figure 1 shows the cyclic voltammetry for TMPD and BF at Pt and at MoS_2 in the dark or illuminated with a 5-mW, beam-expanded, 632.8-nm He-Ne laser providing ~50 mW/cm^2 optical power. The anodic peak positions are listed in Table I. Note that both TMPD and BF exhibit two, reversible, one-electron waves at Pt[7,8] but at MoS_2 in the dark there is only one, reversible, one-electron wave under the same conditions and at the same potential as at Pt. This result shows that the first oxidation has an $E°$ situated in the conduction band but that the second $E°$ is between E_{VB} and E_{CB}. Upon illumination, MoS_2 exhibits two waves, one at the same position as in the dark and the other somewhat more positive and somewhat broader than the first wave. The second, light-dependent wave on MoS_2 is logically associated with the uphill oxidation of $TMPD^+$ to $TMPD^{2+}$ or BF^+ to BF^{2+}. Quite interestingly, the dark wave for BF and the second wave are separated by only ~150 mV; within the framework of the model developed above, this places E_{FB} between the two peak positions. The onset of the photocurrent for both TMPD and BF is at approximately +0.3 V as seen in Figure 1. We thus bracket E_{FB} between +0.3 and +0.5 V and assign it the value of +0.30 + 0.05 V vs. SCE. Essentially the same results are found in EtOH solvent, but for both TMPD and BF there appear to be adsorption phenomena associated with the second oxidation wave. Further, it is interesting to note that our value of E_{FB} is close to that given for aqueous media.[4]

The one-electron reductant ferrocene behaves consistently; sluggish oxidation obtains in the dark at MoS_2, despite the fact that the formal potential is only 80 mV more positive than for BF^+/BF, Table I. The wave for ferrocene is broader and the peak-to-peak separation is much greater than at Pt. Oxidation of acetylferrocene, 1,1'-diacetylferrocene, and $[Ru(2,2'\text{-bipyridine})_3]^{2+}$ is not found at MoS_2 in the dark but each can be oxidized in an uphill sense upon illumination of MoS_2, Table 1. For example, the oxidation of $[Ru(2,2'\text{-bipyridine})_3]^{2+}$ occurs ~0.5 V more negative than at Pt.

All of the reductants examined thus far exhibit a photoanodic current onset in the vicinity of +0.30 V vs. SCE, consistent with the assigned value of E_{FB}. However, we do find that the photoanodic current peak is not at the same position for all of the redox couples employed. Some of the variations may be due to minor variations in the electrodes used, but an explanation is required for the rather large difference between

Table I. Comparison of Anodic Peak Current Positions for Various Redox Couples at Pt and n-Type MoS_2[a]

reductant; A,A$^+$	electrode	V vs. SCE E°[b]	$E_{PA}(A^+/A)$	$E_{PA}(A^{2+}/A^+)$
TMPD, TMPD$^+$	Pt	0.10, 0.68	0.14	0.82
	MoS_2 (dark)		0.15	not obsd
	MoS_2 (light)		0.15	0.58
BF, BF$^+$	Pt	0.30, 0.67	0.34	0.67
	MoS_2 (dark)		0.34	not obsd
	MoS_2 (light)		0.34	0.50
ferrocene	Pt	0.38	0.42	
	MoS_2 (dark)		0.50 (broad)[c]	
	MoS_2 (light)		0.48	
acetylferrocene	Pt	0.63	0.66	
	MoS_2 (dark)		not obsd	
	MoS_2 (light)		0.54	
1,1′-diacetyl-ferrocene	Pt	0.83	0.87	
	MoS_2 (dark)		not obsd	
	MoS_2 (light)		0.59	
[Ru(2,2′-bipyridine)$_3$]$^{3+/2+}$	Pt	1.25	1.30	
	MoS_2 (dark)		not obsd	
	MoS_2 (light)		0.83	

[a] All data are for CH_3CN/0.1 M [n-Bu_4N]ClO_4 solutions at 25 °C. Pt and MoS_2 data for a given reductant were recorded in the same solution. Reductants are at ~1 mM concentration in each case. E_{PA} is the position of the anodic current peak; TMPD is N,N,N',N'-tetramethyl-p-phenylenediamine; BF is biferrocene. Illumination of n-type MoS_2 was with 632.8-nm light from a He-Ne laser (~50 mW/cm^2). [b] These E°'s are from cyclic voltammetry at Pt-foil electrodes in the electrolyte solution used for all other studies. [c] See text.

the +0.83 for [Ru(2,2′-bipyridine)$_3$]$^{3+/2+}$ compared with the +0.5 to +0.6 for the other couples. We attribute the differences in photoanodic peak positions to surface states between E_{VB} and E_{CB} which facilitate the reduction of solution species. Evidence for surface states comes from the observation that BF^{2+}, TMPD^{2+}, 1,1′-diacetylferricenium, acetylferricenium, and [Ru(2,2′-bipyridine)$_3$]$^{3+}$ all undergo reduction at n-type MoS_2 in the dark at potentials which are positive of E_{FB}.[1-3] Crudely, we find that at a given sweep rate the reduction peak in the dark is more positive as the E° of the system in question becomes more positive. Often when low concentrations of the oxidized form are involved, the reduction peak in the dark at n-type MoS_2 occurs near the position found at Pt at ~100 mV/s sweep rates. Low concentrations are important since only low current densities are required to see the cyclic voltammetric wave. Apparently, the surface state density is sufficiently low that the reduction current can be overcome at even modest hole generation rates (low light intensity). The ~50 mW/cm^2 light intensity employed here is of the same order of magnitude as that expected from sunlight. Generally, we find that increased light intensity makes the cyclic waves sharper and results in more negative photoanodic current peaks, but the peak is never found more negative than +0.45 V and the onset is no more negative than +0.30 V vs. SCE.

The redox couples investigated and listed in Table I are chosen, in part, because they have fast charge transfer kinetics. But a priori we really do not know whether the kinetics will be as favorable at an electrode material such as MoS_2. Therefore, it is possible that the variation in the photoanodic peak position is attributable, at least in part, to the differences among the couples in their heterogeneous electron-transfer rate at MoS_2. The relationship between surface states, the rate of photooxidation, and dark reduction, and the nature of the solution species is not clear.

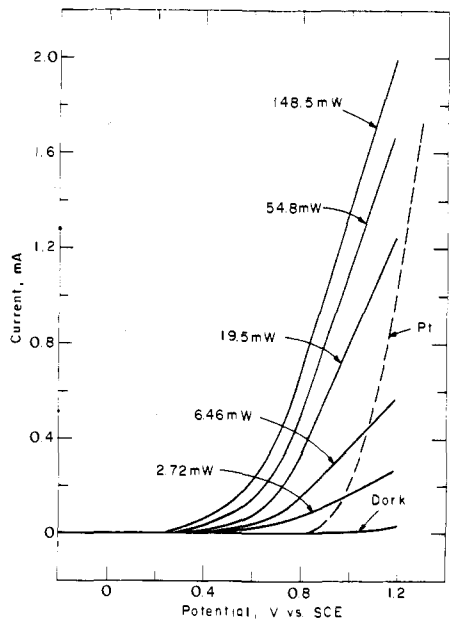

Figure 2. Representative equilibrium current-voltage curves (5 mV/s) for n-type MoS_2 in 0.1 M [Et_4N]Cl/0.1 M [n-Bu_4N]ClO_4/CH_3CN electrolyte. Incident 514-nm optical power is given in mW; to obtain light intensity or current density, multiply by 15 cm^{-2}. The current-voltage curve for a Pt wire electrode of similar area to the MoS_2 electrode is shown for comparison (dashed curve).

Sustained Oxidation of Cl$^-$ in Nonaqueous Media. With a band gap of 1.75 eV, the position of E_{VB} for MoS_2 is at a very positive potential, ~1.9 V vs. SCE. Accordingly, visible light generation of holes in MoS_2 could lead to oxidation processes as difficult energetically as those which can be effected by ultraviolet light illumination of the very durable n-type TiO_2 ($E_{VB} \approx +2.0$ V vs. SCE).[9] One question is whether such processes do occur, and if so, for how long and with what electrical energy savings by using light. From the data in Table I it is obvious that there are a large number of species that can be oxidized at illuminated, n-type MoS_2. However, a number of these systems cannot be oxidized with constant efficiency; that is, at a fixed potential where photocurrent does obtain, the photocurrent declines in time. The difficulties would appear to arise from the redox couples used in that the MoS_2 becomes covered with precipitates from either the starting material or from the electrochemical product. Refreshing the electrode surface by rinsing with a suitable solvent does rejuvenate the photocurrent, but it would appear that MoS_2 photoanodes suffer the same sorts of difficulties that are encountered generally in organic electrochemistry where solid electrodes are employed. In these instances, it is difficult to determine just how durable the MoS_2 actually is. Accordingly, we sought to find a redox system which could be studied in CH_3CN electrolyte solution in order to assess the durability of n-type MoS_2. The powerful oxidizing power of photogenerated holes suggested that we attempt the oxidation of Cl$^-$.

In CH_3CN electrolyte solution Cl$^-$ is susceptible to sustained photooxidation at n-type MoS_2. Essentially the same findings obtain with LiCl or [Et_4N]Cl. Figure 2 shows the steady-state photocurrent-voltage curves for a solution con-

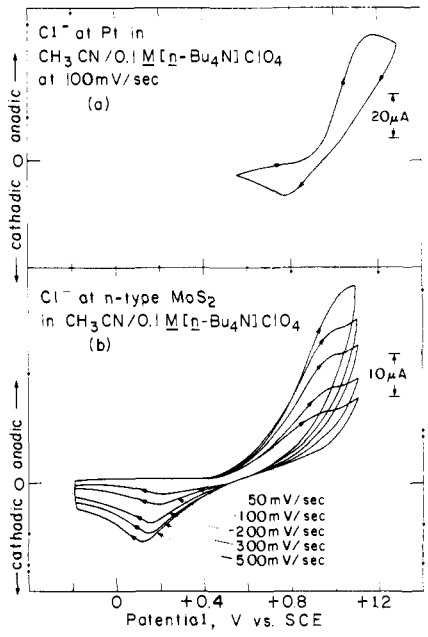

Figure 3. Comparison of cyclic voltammetry for 0.5 mM $[Et_4N]Cl$ at Pt and illuminated MoS_2 at 632.8 nm, ~50 mW/cm².

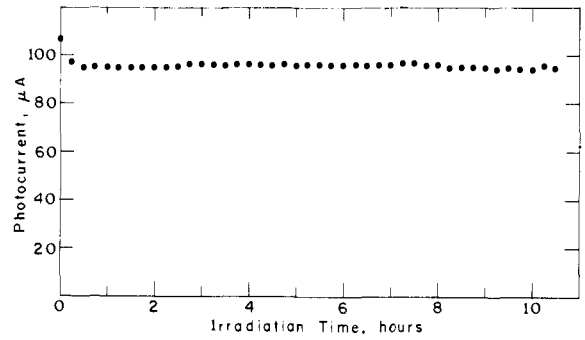

Figure 4. Plot of photocurrent against time for n-type MoS_2 (~0.1 cm²) illuminated with 632.8-nm light (~50 mW/cm²). The electrode was immersed in a stirred CH_3CN solution of 0.1 M $[Et_4N]Cl$ and 0.1 M $[n\text{-}Bu_4N]ClO_4$. The electrode potential was fixed at +0.9 V vs. SCE.

taining Cl^-. In the CH_3CN/0.1 M $[n\text{-}Bu_4N]ClO_4$ solution, no photocurrent is found over the potential range scanned. The oxidation current at a Pt electrode is shown for comparison. The oxidation of Cl^- at Pt is known to produce Cl_2/Cl_3^- mixtures.[10] At n-type MoS_2 the photocurrent onset for Cl^- oxidation is near +0.3 V vs. SCE, consistent again with the value of E_{FB} determined from cyclic voltammetry.

It would appear that the oxidation of Cl^- can be effected in an uphill sense at illuminated n-type MoS_2 since the onset of oxidation current is at a more positive potential at the Pt electrode. By "uphill" we mean the oxidation occurs at potentials more negative than found at a reversible electrode. But it is the oxidizing power of the photogenerated holes that makes possible the uphill process. Cyclic voltammetry, Figure 3, of Cl^- oxidation at Pt and at illuminated n-type MoS_2 reveals that the photoanodic peak for Cl^- oxidation is at a more negative potential than the anodic peak found at Pt. At increased light intensity, the photoanodic peak is observed to be as negative as +0.72 V vs. SCE. From the onset potentials for oxidation current, it would appear that illumination of an n-type MoS_2 photoanode allows an electrical energy savings of >0.5 V compared with a Pt anode for Cl^- oxidation.

The data summarized for Cl^- photooxidation accord well with that for the various couples detailed in Table I. Moreover,

Table II. Representative Output Characteristics for an n-Type MoS_2-Based Photoelectrochemical Cell[a]

input, mW[b]	Φ_e[c]	max power output, μW[b]	max V (V at η_{max})[d]	η_{max}, %[e]
0.660	0.20	3.40	400 (170)	0.52
2.90	0.13	7.20	400 (120)	0.24
8.62	0.074	12.6	440 (120)	0.15
27.0	0.038	22.8	470 (120)	0.084
80.9	0.017	33.1	510 (120)	0.041
183	0.009	43.7	530 (140)	0.024

[a] All data for CH_3CN/0.1 M $[n\text{-}Bu_4N]ClO_4$/0.2 M $[Et_4N]Cl$ with Cl_2 added to bring E_{redox} to +0.82 V vs. SCE. [b] Input power is the 514-nm line from a Spectra-Physics argon-ion laser. For power density, multiply by 56 cm⁻². [c] Quantum yield for electron flow at E_{redox}; this corresponds to the short-circuit quantum yield taken to be the number of electrons passed per incident photon. [d] Maximum voltage is the open-circuit photopotential and the value in parentheses is the output voltage at the maximum power point in millivolts. [e] Efficiency for conversion of 514-nm light to electricity.

we find the photoanodic current for Cl^- oxidation to be remarkably constant. Figure 4 shows a representative plot of photocurrent against time for Cl^- oxidation. A constant (within 3%) photocurrent of ~1 mA/cm² is shown for a period exceeding 10 h. In a subsequent experiment with the same electrode, 8 h of constant (within 3%) photocurrent was found at ~10 mA/cm². Similar experiments have been carried out with other MoS_2 photoelectrodes and the results are essentially invariant. The surfaces of MoS_2 electrodes used in such media are not visibly changed, and the photocurrent-voltage properties are constant as well. For a number of MoS_2 electrodes, we have passed a significantly larger number of moles of electrons through the interface than the number of moles of MoS_2 initially used. No evidence for destruction of MoS_2 obtains.

The photooxidation of Cl^- results in the generation of Cl_2/Cl_3^-, as with oxidation at Pt. Several facts establish the product identity. Photoxidation of Cl^- in the MoS_2 anode compartment of a two-compartment cell results in a yellow coloration of the solution. The characteristic smell of Cl_2 is present after photooxidation, and the solution gives a positive starch/iodine test. The anolyte potential moves from ~0.0 to ~+0.8 V vs. SCE or very close to the value obtained by adding Cl_2 to the solution. Addition of the anolyte product solution to a solution of $[IrCl(CO)(PPh_3)_2]$ results in the apparent oxidation to an Ir(III) compound.[11] Thus, it would appear that n-type MoS_2 can be used to effect the sustained uphill generation of Cl_2 by using visible light. Given that the band gap of MoS_2 is only 1.75 eV, the ~0.5 V output voltage for Cl_2 production is respectable. However, the rectangularity of the photocurrent-voltage curves is poor, Figure 2, and the overall efficiency of a light-driven process is small. Further, the quantum yield for electron flow is small, and the quantum yield declines with increasing light intensity. Table II summarizes some of the quantitative information culled from an electrochemical cell. The important finding is that the MoS_2 is rugged; a $CH_3CN/Cl_2/Cl^-$ system comprises an electrolyte solution which yields a stable photocurrent from MoS_2. In a single compartment cell, we have demonstrated that an n-type MoS_2-based photocell can be operated by using the Cl_2/Cl^- couple. On the time scale of our experiments, we found no evidence for chlorination of the organic matter in the cell, but ultimately such would likely obtain. The Cl_2/Cl^- couple would be too corrosive for long duration experiments. But interestingly, it is not the stability of illuminated MoS_2 which is limiting.

The durability of MoS_2 is especially interesting when contrasted to n-type CdS (E_{BG} = 2.4 eV) which has been estab-

lished to have $E_{VB} \approx +1.5$ V vs. SCE.[2] We find that CdS shows substantial anodic decomposition current when illuminated in electrolyte solutions where MoS_2 is stable. In one experiment, for example, n-type CdS illuminated at −0.65 V vs. SCE in the presence of Cl_2/Cl^- such that 2×10^{-5} mol of electrons passed at ~30 mA/cm^2 yields obvious electrode deterioration, while MoS_2 illuminated at +0.8V at the same current density to pass 4×10^{-5} mol of electrons showed no deterioration. Though CdS has energetics which would indicate that Cl_2 generation is possible (E_{VB} more positive than $E°(Cl_2/Cl^-)$), the sustained generation of Cl_2 is not found. Either Cl_2 is never formed or it (or intermediates) attacks the surface of CdS to oxidize it. The CdS-based cell employing an I_3^-/I^- couple is durable,[12] but it is likely that the I_3^-/I^- is about as oxidizing a medium as can be tolerated by CdS-based energetics for the CdS anodic decomposition.[13] It is not clear just what the anodic decomposition energetics are for MoS_2 since the products are not known. But the ability of MoS_2 to survive Cl_2 is remarkable.

Comparison with Aqueous Electrolyte Solutions. n-Type MoS_2 was first characterized in aqueous media; in particular, photocurrent-voltage curves and photocurrent vs. time were recorded in H_2O/0.1 M KCl solutions. The photocurrent onset was in the vicinity of +0.3 V vs. SCE consistent with E_{FB} close to what we find in CH_3CN. Curiously, the earlier characterization of MoS_2 in H_2O/0.1 M KCl did not include the consideration that Cl^- could be oxidized by the photogenerated holes. Such may have been responsible for the relatively stable photocurrents found from the MoS_2. The main finding from our study in this connection is that in the nonaqueous media the energetics are the same as for the H_2O solvent and we do find good, constant current for Cl^- oxidation. Specific adsorption as with I^- affects E_{FB},[4] but we have not found such an effect for the reductants studied in CH_3CN. Preliminary results do show that I^- can be oxidized at a potential more negative than +0.30 V vs. SCE by illumination of MoS_2 in CH_3CN solution.

Summary

The interfacial energetics for n-type MoS_2 contacting CH_3CN electrolyte solutions have been accurately defined by using cyclic voltammetry. The best data concern two-electron redox couples having one reversible, one-electron wave more negative than the flat-band potential, E_{FB}, of MoS_2 and another, light-dependent, one-electron wave having $E°$ more positive than E_{FB}. We find $E_{FB} = +0.30 + 0.05$ V vs. SCE for n-type MoS_2. A large number of reductants can be oxidized in an uphill sense by visible light irradiation of MoS_2; maximum photovoltages are ~0.5 V. The sustained photooxidation of Cl^- at n-type MoS_2 has been demonstrated; optical energy conversion efficiency is low. Improvement hinges on improving the quantum yield and the current-voltage properties. The poor properties encountered thus far are likely due to surface states situated between the valence and conduction band. Evidence for surface states comes from the cyclic voltammetry experiments.

Experimental Section

Materials. A sample of natural, single-crystal MoS_2 was obtained from Climax Molybdenum Co. (Greenwich, Conn.). Samples were cleaved by slipping a sharp steel blade between the layers and then cut into smaller pieces (typically $5 \times 5 \times 0.1$ mm) by pressing the blade perpendicular to the layers. Spectrograde CH_3CN, absolute EtOH, ferrocene, acetylferrocene, LiCl, and $[Et_4N]Cl$ were used as received from commercial sources, after checking for electroactive impurities at a Pt electrode. 1,1′-Diacetylferrocene does show impurities and was purified by column chromatography prior to use. *N,N,N′,N′*-Tetramethyl-*p*-phenylenediamine (TMPD) was purified by sublimation. Biferrocene (BF) was prepared as described in the literature.[8] $[Ru(2,2'\text{-bipyridine})_3]^{2+}$ was used as the ClO_4^- salt. $[n\text{-}Bu_4N]ClO_4$, from Southwestern Analytical Chemicals, was vacuum dried at 70 °C for 24 h.

Electrode Preparation. MoS_2 electrodes (~0.1 cm^2 exposed area) were fabricated as follows. Satisfactory electrical contacts were made by rubbing Ga-In eutectic on one side of a freshly cleaved crystal and mounting (with conducting silver epoxy) onto a coiled copper wire. The copper wire lead was passed through 4-mm Pyrex tubing and the assembly insulated with ordinary epoxy leaving only the MoS_2 001 face exposed to the electrolyte.

MoS_2 is a fragile material. The surface is susceptible to damage from too vigorous stirring which presumably shears off flakes of MoS_2. Also, rough handling can cause the epoxy seal to break loose from the surface resulting in leakage to the metallic mount.

Electrochemical Equipment and General Procedures. Cyclic voltammograms were recorded in CH_3CN or EtOH solutions of 0.1 M $[n\text{-}Bu_4N]ClO_4$ by using a PAR Model 173 potentiostat equipped with a Model 175 programmer. Scans were recorded with a Houston Instruments X-Y recorder. Except where otherwise stated, a single compartment cell was used employing a standard three electrode configuration with a Pt counterelectrode and a saturated calomel reference electrode (SCE). All measurements are for 25 °C.

Electrodes were illuminated by using a beam-expanded, 632.8-nm, He-Ne laser (Coherent Radiation) providing ~50 mW/cm^2 or an Ar ion laser (Spectra Physics Model 164) tuned to the 514-nm line. The intensity of the irradiation was determined by using a Tektronix J16 digital radiometer equipped with a J6502 probe.

Electrodes were routinely checked prior to use and rechecked at the completion of most experiments by scanning in a 0.5 mM TMPD/0.1 M $[n\text{-}Bu_4N]ClO_4/CH_3CN$ electrolyte at 100 mV/s. Under illumination, good electrodes show a photocurrent onset for $TMPD^+ \rightarrow TMPD^{2+}$ at ~0.3 V vs. SCE with a well-defined photoanodic peak at ~0.5 V vs. SCE. The presence of a wave for $TMPD^+/TMPD^{2+}$ in the dark indicates an imperfect epoxy seal and such electrodes were rejected.

Acknowledgments. We thank the Office of Naval Research for partial support of this research. M.S.W. acknowledges support as a Dreyfus Teacher-Scholar Grant recipient, 1975–1980. We appreciate the generous gift of single crystal MoS_2 from Climax Molybdenum Co.

References and Notes

(1) Frank, S. N.; Bard, A. J. *J. Am. Chem. Soc.* **1975**, *97*, 7427.
(2) Kohl, P. A.; Bard, A. J. *J. Am. Chem. Soc.* **1977**, *99*, 7531.
(3) Laser, D.; Bard, A. J. *J. Phys. Chem.* **1976**, *80*, 459.
(4) Tributsch, H.; Bennett, J. C. *J. Electroanal. Chem.* **1977**, *81*, 91. For related work, see Tributsch, H. *J. Electrochem. Soc.* **1978**, *125*, 1086. *Ber. Bunsenges. Phys. Chem.* **1977**, *81*, 361; **1978**, *82*, 169. Gobrecht, J.; Tributsch, H.; Gerischer, H. *J. Electrochem. Soc.* **1978**, 125, 2085.
(5) Nozik, A. J. *Annu. Rev. Phys. Chem.* **1978**, *29*, 189.
(6) The model for the semiconductor/liquid junction detailed in Scheme I follows from the treatment in Gerischer, H. *J. Electroanal. Chem.* **1975**, *58*, 263.
(7) Yao, T.; Musha, S.; Munemori, M. *Chem. Lett.* **1974**, 939.
(8) Morrison, W. H., Jr.; Krogsrud, S.; Hendrickson, D. N. *Inorg. Chem.* **1973**, *12*, 1998.
(9) The position of E_{VB} in CH_3CN solution of +2.0 V vs. SCE is from ref 1 and a number of interesting oxidations can be effected by illuminated TiO_2: Frank, S. N.; Bard, A. J. *J. Am. Chem. Soc.* **1977**, *99*, 4667.
(10) (a) Kolthoff, I. M.; Coetzee, J. F. *J. Am. Chem. Soc.* **1957**, *79*, 1852. (b) Mann, C. K.; Barnes, K. K. "Electrochemical Reactions in Non-Aqueous Media", Marcel Dekker: New York, 1970.
(11) Vaska, L. *Acc. Chem. Res.* **1968**, *1*, 335.
(12) Nakatani, K.; Matsudaira, S.; Tsubomura, H. *J. Electrochem. Soc.* **1978**, *125*, 406.
(13) Bard, A. J.; Wrighton, M. S. *J. Electrochem. Soc.* **1977**, *124*, 1706.